Topological Modifications for Performance Improvement and Size Reduction of Wideband Antenna Structures

Adrian Bekasiewicz[1]
[1] Faculty of Electronics, Telecommunications and Inf.
Gdansk University of Technology
Gdansk, Poland
bekasiewicz@ru.is

Slawomir Koziel[1,2]
[2] Engineering Optimization & Modeling Center
Reykjavik University
Reykjavik, Iceland
koziel@ru.is

Abstract—**Compact antennas belong to the key components of modern communication systems. Their miniaturization is often achieved by introducing appropriate topological changes such as simple ground plane slots or tapered feeds. More sophisticated modifications are rarely considered in the literature because they normally lead to significant increase of the number of tunable parameters, which makes the antenna design process more challenging. On the other hand, complex topological changes are questionable as their effects on radiator performance and/or size reduction are difficult to be verified in practice. In particular, parameter sweeping commonly used for dimension adjustment is incapable of their appropriate handling. In this work, the effect of feed line and ground plane modifications on performance and size reduction of a wideband antenna is investigated. Considered geometrical changes include a ground plane slot and a stepped-impedance feed line (both with gradually increasing number of sections). The modified structures have been optimized for minimum in-band reflection and minimum size using a robust gradient-based algorithm. The obtained results demonstrate that complex topological modifications may be useful for achieving both good performance and small size when handled comprehensively.**

Keywords—compact antenna design; EM-driven design; antenna miniaturization; topology modifications; computer-aided design

I. INTRODUCTION

Small size is an important prerequisite for antenna structures utilized within modern communication systems. Compact radiators are of key importance for handheld/wearable devices, sensor networks, and internet of things applications [1]-[3]. Although compact dimensions are easier to be obtained for certain antenna classes such as monopoles [4], or slot radiators [5], they can be also achieved by introducing geometrical changes into the structure topology [6]-[8]. In most cases, the aim of such modifications is to ensure an acceptable impedance bandwidth for the miniaturized radiator [8], [9]. However, they can be also utilized to secure other performance-related properties, such as band-pass or band-stop behavior [7], [10]. The mentioned topological changes significantly increase complexity of the antenna structures [5], [9]. One of the consequences is that computationally expensive full-wave electromagnetic (EM) simulations are mandatory for their reliable evaluation.

High evaluation cost makes antenna design a challenging process. Conventional approaches are heavily based on engineering experience, where the radiator geometrical dimensions are determined through interactive adjustment of the parameter values followed by visual inspection of structure responses [5], [8], [11]. As shown in [12], such an approach cannot ensure that truly optimum design will be found. Other downsides of the manual design include limited flexibility: parameter sweeps can only handle one performance figure (typically, an antenna in-band reflection); also, the method cannot effectively control more than one parameter at a time. This is a serious limitation as compact antenna structures are often characterized by over a dozen geometrical variables [5], [9], [13], all of which have to be adjusted simultaneously [14]. From this perspective, numerical optimization is the only reliable tool for miniaturized radiator design [12], [14].

Antenna design is an inherently multi-objective task, where certain conflicting figures related to the structure size and/or performance have to be improved at the same time [14], [15]. In case the designer priorities are not clearly defined, the problem needs to be handled using genuine multi-objective optimization. The latter produces a set of the best trade-off solutions that are attainable for the antenna at hand [14], [16]. Otherwise, the design requirements can be aggregated to a single-objective using, e.g., a weighted sum function. Alternatively, a primary objective can be specified whereas requirements concerning the remaining figures can be controlled through suitably defined penalty functions [17]. As indicated in [9], [12], [17], the latter approach is particularly useful for miniaturization of antenna structures.

Despite usefulness of numerical optimization for obtaining high performance and/or small antenna size, the overall success of the design process depends on the designer who (based on the experience) has to manually select topological modifications required to obtain a desired functionality [8]. Normally, this is realized by implementing changes which are known for their usefulness in high performance and/or small size radiators. The most popular ones include slits below the feed line [12], L- and I-shaped ground plane stubs [7], [18]

slots within the radiating element [19], as well as tapered or stepped impedance feed lines [7]. Such modifications and their combinations allow for obtaining structures with footprints smaller than 200 mm² [5], [9]. On the other hand, due to the lack of appropriate design tools, more complex topology modifications as multi-stage feed lines, or folded stubs are rarely considered in the literature [9], [14].

In this work, the effect of topological modifications on the performance and the size of a compact wideband monopole antenna is investigated. Specifically, we consider the ground plane slots and the feed line changes in the context of improving the in-band reflection and reduction of structure footprint. The numerical tests have been performed for four antenna variants, i.e., without modifications and with a gradually increasing number of ground plane slot and feed line sections. The obtained results indicate that the increased number of sections (and hence degrees of freedom) significantly affects the antenna properties (both performance- and size-wise).

II. CASE STUDIES: COMPACT MONOPOLE ANTENNA

Consider antenna topologies shown in Fig. 1 [19]. All the structures are implemented on a 1.55 mm thick FR-4 substrate ($\varepsilon_r = 4.3$ tanδ = 0.025). They consist of a rectangular radiator with two vertical slots driven by a 50 Ohm microstrip line. The reference structure of Fig. 1(a) is characterized by a rectangular ground plane and a plain feed. As shown in Figs. 1(b)-(d), modifications of the remaining antennas include introduction of ground plane slots and stepped-impedance feeds. The vector of design parameters describing the radiator part, $\boldsymbol{x}_r = [d\ w_s\ l_s\ o_1\ o_2]^T$, is the same for all structures. Variable vectors representing the feed and the ground plane for Antennas I (cf. Fig. 1(a)) through IV (cf. Fig. 1(d)) are $\boldsymbol{x}_{f1} = [l_{g0}\ l_{t0}]^T$, $\boldsymbol{x}_{f2} = [\boldsymbol{x}_{f1}\ l_{g1}\ w_{g1}\ l_{t1}\ w_{t1}]^T$, $\boldsymbol{x}_{f3} = [\boldsymbol{x}_{f2}\ l_{g2}\ w_{g2}\ l_{t2}\ w_{t2}]^T$, and $\boldsymbol{x}_{f4} = [\boldsymbol{x}_{f3}\ l_{g3}\ w_{g3}\ l_{t3}\ w_{t3}]^T$, respectively. The combined sets of adjustable parameters for the radiators are given by $\boldsymbol{x}_k = [\boldsymbol{x}_r\ \boldsymbol{x}_{f.k}]^T$, $k = 1, 2, 3, 4$; $w_{t0} = 3$ remains fixed to ensure 50 Ohm input impedance. The unit for all geometry parameters is mm. The antennas are implemented in CST Microwave Studio and simulated using its time domain solver [20]. For the sake of reliable evaluation all considered EM models are equipped with SMA connectors.
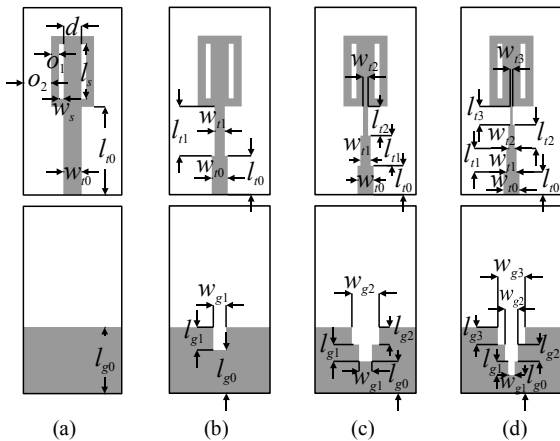

Fig. 1. Topologies of the considered monopole: (a) Antenna I, (b) Antenna II, (c) Antenna III, and (d) Antenna IV.

Footprints of the considered antennas are defined as $A_k(\boldsymbol{x}) = A_0 \times B_k$, where $A_0 = 2(o_1 + o_2 + w_s) + d$ is common for all structures. The radiators heights are as follows: $B_1 = 2o_1 + o_2 + l_s + l_{t0}$, $B_2 = B_1 + l_{t1}$, $B_3 = B_2 + l_{t2}$, and $B_4 = B_3 + l_{t3}$ (see Fig. 1), for Antennas I to IV, respectively. The lower and upper bounds for the radiator part are $\boldsymbol{l}_{br} = [1\ 0.2\ 4\ 0.5\ 1]^T$ and $\boldsymbol{u}_{br} = [7\ 2\ 14\ 3\ 5]^T$. For the Antenna I the feed-related bounds are $\boldsymbol{l}_{bf.1} = [4\ 2]^T$ and $\boldsymbol{u}_{bf.1} = [11\ 14]^T$, whereas for the remaining structures they are given as $\boldsymbol{l}_{bf.k} = [0.2\ 0.2\ 1\ 1]^T$ and $\boldsymbol{u}_{bf.k} = [4.2\ 4\ 10\ 4]^T$.

III. METHODOLOGY

In this section, we describe the utilized design optimization methodology. Specifically, we formulate the design problem and define the design specifications for antenna optimization w.r.t. minimum in-band reflection and size reduction, respectively. Moreover, we briefly describe the optimization algorithm. Numerical results and discussion are provided in Section IV.

A. Problem Formulation and Specifications

Let $\boldsymbol{R}(\boldsymbol{x})$ be the EM model response of the antenna structure at hand obtained for the given vector of design parameters $\boldsymbol{x}$. The design problem can be formulated as the following minimization task

$$\boldsymbol{x}^* = \arg \min_{\boldsymbol{x}} U(\boldsymbol{x}) \qquad (1)$$

where $U(\boldsymbol{x})$ is a scalar objective function and $\boldsymbol{x}^*$ is the optimal design to be found. Here, we consider two design cases, i.e., minimization of the antenna in-band reflection and footprint reduction while ensuring acceptable electrical performance. The objective function for the first case is given as

$$U(\boldsymbol{x}) = S(\boldsymbol{x}) = \max\{|S_{11}(\boldsymbol{x})|_{3.1\,\mathrm{GHz\,to\,10.6\,GHz}}\} \qquad (2)$$

where $S_{11}(\boldsymbol{x}) = \boldsymbol{R}(\boldsymbol{x})$ is the antenna reflection. For the second case, the design objective is defined as follows [9]

$$U(\boldsymbol{x}) = U(A(\boldsymbol{x}), S(\boldsymbol{x})) = A(\boldsymbol{x}) + \beta \cdot c(S(\boldsymbol{x}))^2 \qquad (3)$$

Here, $A(\boldsymbol{x})$ is the antenna size (cf. Section II), whereas $S(\boldsymbol{x})$ is as in (2). The penalty component $c(S(\boldsymbol{x})) = \max\{(S(\boldsymbol{x}) + 10)/10, 0\}$ enforces the maximum in-band reflection to be around the level of -10 dB towards the end of the optimization process. The contribution of the penalty term in (3) is controlled using the penalty factor β (here, $\beta = 10$).

B. Optimization Algorithm

Design problems formulated in Section III.A are challenging. Moreover, the number of adjustable parameters for the considered antenna structures vary from 7 to 19 (cf. Section II). Therefore, a robust optimization method is required for their successful optimization. Here, we use a gradient-based algorithm embedded in a trust-region framework [21]. It generates a series of approximations $\boldsymbol{x}^{(i)}$, $i = 0, 1, \ldots$ to the solution $\boldsymbol{x}^*$ of the original problem (1) as

$$\boldsymbol{x}^{(i+1)} = \arg \min_{\boldsymbol{x}:\|\boldsymbol{x}-\boldsymbol{x}^{(i)}\|\leq\delta^{(i)}} U\left(\boldsymbol{G}^{(i)}(\boldsymbol{x})\right) \qquad (4)$$

where $G^{(i)}$ is the linear expansion model given by

$$G^{(i)}(x) = R(x^{(i)}) + J(x^{(i)}) \cdot (x - x^{(i)}) \qquad (5)$$

Here, J is a Jacobian of R obtained through finite differentiation. The trust-region radius $\delta^{(i)}$ is updated using the standard rules based on a gain ratio (i.e., actual versus predicted improvement of the objective function [21]). The initial radius is $\delta^{(0)} = 1$. It should be noted that, for successful iterations, the computational cost of the algorithm is only $N + 1$ EM model evaluations (with N being the number of antenna parameters) per iteration. Each unsuccessful step requires additional EM simulations. For more detailed description of algorithm see, e.g., [21], [22].

IV. NUMERICAL RESULTS AND DISCUSSION

The initial design for Antenna I is set to $x_{\mathrm{I.1}}^{(0)} = [3.9 \ 0.35 \ 9.5 \ 1.6 \ 2.5 \ 9 \ 13]^T$. The final design $x_{\mathrm{I.1}}^* = [5.6 \ 0.23 \ 8.74 \ 1.63 \ 4.99 \ 10.61 \ 13.52]^T$ has been obtained using (2) after 10 iterations of the algorithm of Section III.B. It should be noted that the in-band reflection of the optimized structure is only -8.7 dB which violates the -10 dB performance threshold (cf. Section III.A) Therefore, the second design case has not been considered for Antenna I. The initial designs for Antennas II to IV are based on $x_{\mathrm{I.1}}^{(0)}$. For the second structure, the final design $x_{\mathrm{I.2}}^* = [4.01 \ 0.21 \ 8.71 \ 1.3 \ 4.5 \ 8.04 \ 5.99 \ 2.5 \ 1 \ 8.08 \ 1.64]^T$ has been obtained after 8 algorithm iterations. The maximum in-band reflection of the final design is -14.5 dB, whereas its size is 480 mm². The optimized parameter vector for Antenna III $x_{\mathrm{I.3}}^* = [4.8 \ 0.2 \ 9.9 \ 0.73 \ 4.97 \ 8.03 \ 5.85 \ 1.14 \ 3.31 \ 3.84 \ 1.8 \ 1.26 \ 1.23 \ 4.3 \ 1.69]^T$ has been obtained in 7 iterations of (5). Its in-band reflection and size are -14.25 dB and 504 mm², respectively. Finally, the optimized dimensions of Antenna IV $x_{\mathrm{I.4}}^* = [5.94 \ 0.2 \ 7.47 \ 1.46 \ 5 \ 9.66 \ 2.01 \ 0.27 \ 1.4 \ 6.08 \ 2.59 \ 0.36 \ 3.99 \ 3.02 \ 1.03 \ 0.31 \ 1.82 \ 4.95 \ 3.97]^T$ (reflection of -16.8 dB, size of 606 mm²) have been found after 10 iterations. The electrical and field characteristics of the antennas at their optimized designs are shown in Fig. 2(a) and Fig. 3(a), respectively.

The designs $x_{\mathrm{I.2}}^*$ to $x_{\mathrm{I.4}}^*$ have been used as starting points for the second design case (radiators miniaturization). The optimized parameter vector for Antenna II, $x_{\mathrm{II.2}}^* = [2.98 \ 0.2 \ 7.9 \ 0.8 \ 2.88 \ 7.61 \ 5.83 \ 2.42 \ 1.01 \ 7.87 \ 1.33]^T$, has been found using (3) after 13 iterations of the algorithm of Section III.B. The size of the miniaturized structure is 281 mm², 41% smaller compared to design $x_{\mathrm{I.2}}^*$. For Antenna III, the final design $x_{\mathrm{II.3}}^* = [4.04 \ 0.72 \ 5.96 \ 0.5 \ 1 \ 9.42 \ 5.08 \ 0.91 \ 3.27 \ 2.74 \ 1.87 \ 0.75 \ 1.45 \ 7.71 \ 1]^T$ has been found after 19 iterations. The resulting structure size is only 199 mm² which is 60% smaller compared to design optimized w.r.t. minimum in-band reflection. Finally, the dimensions of miniaturized Antenna IV, $x_{\mathrm{II.4}}^* = [3.21 \ 0.2 \ 4.43 \ 0.5 \ 1.31 \ 9.24 \ 2.02 \ 0.23 \ 1.43 \ 5.23 \ 2.13 \ 0.44 \ 4 \ 5.68 \ 0.5 \ 0.33 \ 1.88 \ 3.95 \ 3.82]^T$, (footprint of 171 mm²) have been found in 13 iterations of (4). Reflection characteristics of the antenna structures obtained for the second design case are compared in Fig. 2(b). It should be noted that all the optimized designs slightly violate the imposed threshold concerning acceptable in-band reflection level (around -9.9 dB instead of -10 dB). This is normal and stems from utilization of the penalty function approach to

enforce the reflection constraint. The radiation patterns of the optimized antennas are given in Fig. 3(b). The results indicate that size reduction results in improved omnidirectionality of the patterns. At the same time, the field characteristics of miniaturized structures are similar. Table I shows comparison of the optimized antennas in terms of electrical performance and size, whereas topologies of radiators optimized for the first and second case are compared in Fig. 4.
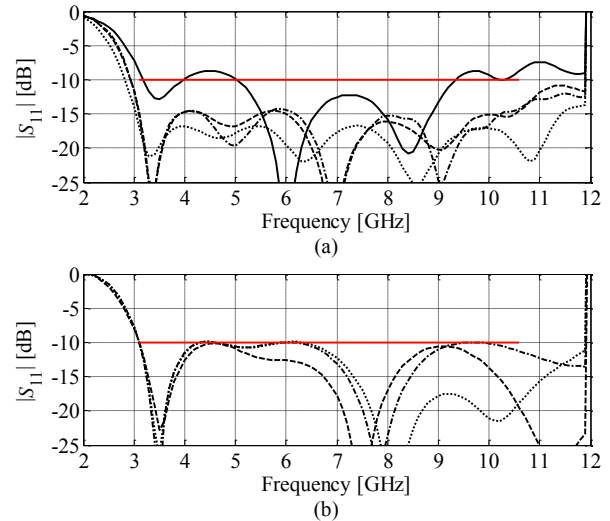

(a)

(b)

Fig. 2. Reflection characteristics of considered antenna structures at the optimized designs: (a) $x_{\mathrm{I.1}}^*$ (—), $x_{\mathrm{I.2}}^*$ (– –), $x_{\mathrm{I.3}}^*$ (–·), $x_{\mathrm{I.4}}^*$ (····), and (b) $x_{\mathrm{II.2}}^*$ (– –), $x_{\mathrm{II.3}}^*$ (–·), $x_{\mathrm{II.4}}^*$ (····).
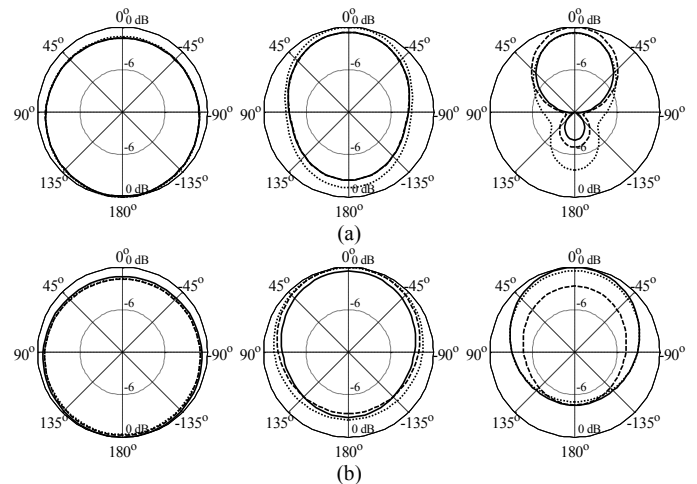

(a)

(b)

Fig. 3. Radiation pattern characteristics obtained for Antennas II (—), III (– –), and IV (····) for the first (a) and the second (b) design case at (from left to right): 4 GHz, 7 GHz, and 10 GHz.
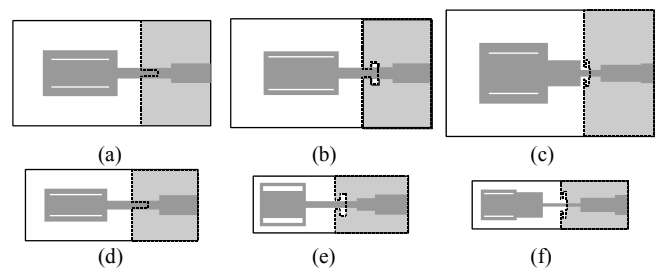

Fig. 4. Antennas II through IV (in scale) optimized for the first design case: (a) $x_{\mathrm{I.2}}^*$, (b) $x_{\mathrm{I.3}}^*$, and (c) $x_{\mathrm{I.4}}^*$, as well as for the second design case: (d) $x_{\mathrm{II.2}}^*$, (e) $x_{\mathrm{II.3}}^*$, and (f) $x_{\mathrm{II.4}}^*$. Dashed lines denote edge of ground planes.

TABLE I COMPARISON OF OPTIMIZED ANTENNA DESIGNS

Design	Case I			Case II			
	Size [mm × mm]	Size [mm²]	max($\|S_{11}\|$) [dB]	Size [mm × mm]	Size [mm²]	max($\|S_{11}\|$) dB	Size reduction* %
I	19.3 × 30.5	588	−8.72	N/A	N/A	N/A	N/A
II	16.1 × 29.9	480	−14.57	10.7 × 26.1	281	−9.91	52.2
III	16.6 × 30.3	504	−14.25	8.5 × 23.5	199	−9.94	65.7
IV	19.3 × 31.5	606	−16.76	7.2 × 23.6	171	−9.89	70.9

* w.r.t. Antenna I, i.e., conventional structure optimized for matching (case I)

The optimization results show that the slot below the feed line (for Antennas III and IV) is narrower towards the edge of the ground plane (see Fig. 4). This indicates that more relaxed changes of slot dimensions from the edge to the interior might improve the impedance bandwidth of a compact radiator (cf. Fig. 2). Another observation is that, for multi-section feed shown in Figs. 4(c) and 4(f), the improved impedance matching and small size have been achieved using low-impedance close-to-radiator section. Besides contribution to matching, the low-impedance section also acts as a radiating element. Consequently, the improvement of pattern characteristics in terms of their omnidirectional behavior can be observed (cf. Fig. 3(a)). It should be also noted that for the first design case, a larger number of parameters results in the increase of antenna sizes. However, it also allows for obtaining smaller designs when optimizing for size reduction.

V. CONCLUSION

In the paper, the effect of feed line and ground plane modifications on the behavior of a compact wideband antenna structure has been investigated based on a series of numerical experiments. Two test cases concerning optimization w.r.t. minimization of in-band reflection and reduction of radiator size have been considered. The tests have been performed for a set of structures characterized by an increased number of sections within the mentioned modifications. The reference antenna (without topological changes) failed at achieving the required −10 dB level of maximum in-band reflection. The remaining radiators have been optimized considering both test cases. The in-band reflection levels and sizes of the obtained antennas vary between −14.3 dB to −16.5 dB and between 281 mm² to only 171 mm², respectively. The results indicate that by increasing the number of sections (and consequently, the number of parameters) electrical performance of structures can be improved. At the same time, for larger number of dimensions, smaller geometries can be obtained while maintaining acceptable electrical performance. The future work will focus on analyzing the effects of other topological changes on size and performance of antenna structures. Estimation of the upper boundary for the number of sections that permits improvement of radiator properties (both performance- and size-wise) will be also investigated.

ACKNOWLEDGMENT

REFERENCES

[1] M. Ur-Rehman, Q.H. Abbasi, M. Akram, and C. Parini, "Design of band-notched ultra wideband antenna for indoor and wearable wireless communications," *IET Microwaves, Ant. Prop.*, vol. 9, no. 3, pp. 243-251, 2015.

[2] G. Li, Y. Huang, G. Gao, X. Wei, Z. Tian, and L.A. Bian, "A handbag zipper antenna for the applications of body-centric wireless communications and Internet of Things," *IEEE Trans. Ant. Prop.*, vol. 65, no. 10, pp. 5137-5146, 2017.

[3] H. Zhou, J. Geng, W. Zhu, J. Li, X. Liang, and R. Jin, "Wideband circularly polarized UHF crossed monopole antenna with unequal power feed for handheld terminals," IEEE Ant. Wireless Prop. Lett., vol. 16, pp. 2915-2918, 2017.

[4] M.G.N. Alsath and M. Kanagasabai, "Compact UWB monopole antenna for automotive communications," *IEEE Trans. Ant. Prop.*, vol. 63, no. 9, pp. 4204-4208, 2015.

[5] Q.-X. Chu, C.-X. Mao, and H. Zhu, "A compact notched band UWB slot antenna with sharp selectivity and controllable bandwidth," *IEEE Trans. Ant. Prop.*, vol. 61, no. 8, pp. 3961-3966, 2013.

[6] A.K. Gautam, S. Yadav, and B.K. Kanaujia, "A CPW-fed compact UWB microstrip antenna," *IEEE Ant. Wireless Prop. Lett.*, vol. 12, pp. 151-154, 2013.

[7] T. Li, H. Zhai, G. Li, L. Li, and C. Liang, "Compact UWB band-notched antenna design using interdigital capacitance loading loop resonator," *IEEE Ant. Wireless Prop. Lett.*, vol. 11, pp. 724-727, 2012.

[8] D.T. Nguyen, D.H. Lee, and H.C. Park, "Very compact printed triple band-notched UWB antenna with quarter-wavelength slots," *IEEE Ant. Wireless Prop. Lett.*, vol. 11, pp. 411-414, 2012.

[9] A. Bekasiewicz and S. Koziel, "A novel structure and design optimization of compact spline-parameterized UWB slot antenna," *Metrology Meas. Syst.*, vol. 23, no. 4, pp. 637-643, 2016.

[10] M. Bod, H.R. Hassani, and M.M.S Taheri, "Compact UWB printed slot antenna with extra Bluetooth, GSM, and GPS Bands," *IEEE Ant. Wireless Prop. Lett.*, vol. 11, pp. 531-534, 2012.

[11] C.-Y. Huang, and J.-Y. Su, "A printed band-notched UWB antenna using quasi-self-complementary structure," *IEEE Ant. Wireless Prop. Lett.*, vol. 10, pp. 1151-1153, 2011.

[12] S. Koziel and A. Bekasiewicz, "Comprehensive comparison of compact UWB antenna performance by means of multi-objective optimization," *IEEE Trans. Ant. Prop.*, vol. 65, no. 7, pp. 3427-3436, 2017.

[13] L. Wang, L. Xu, X. Chen, R. Yang, L. Han, and W. Zhang, "A compact ultrawideband diversity antenna with high isolation," *IEEE Ant. Wireless Prop. Lett.*, vol. 13, pp. 35-38, 2014.

[14] A. Bekasiewicz and S. Koziel, "Structure and computationally-efficient simulation-driven design of compact UWB monopole antenna," *IEEE Ant. Wireless Prop. Lett.*, vol. 14, pp. 1282-1285, 2015.

[15] L. Lizzi, F. Viani, R. Azaro, and A. Massa, "Optimization of a spline-shaped UWB antenna by PSO," *IEEE Ant. Wireless Prop. Lett.*, vol. 6, pp. 182-185, 2007.

[16] X.-S. Yang, K.T. Ng, S.H. Yeung, and K.F. Man, "Jumping genes multiobjective optimization scheme for planar monopole ultrawideband antenna," *IEEE Trans. Ant. Prop.*, vol. 56, no. 12, pp. 3659-3666, 2008.

[17] S. Koziel and A. Bekasiewicz, *Multi-objective design of antennas using surrogate models*, World Scientific, 2016.

[18] L. Liu, S.W. Cheung, and T.I. Yuk, "Compact MIMO antenna for portable UWB applications with band-notched characteristic," *IEEE Trans. Ant. Prop.*, vol. 63, no. 5, pp. 1917-1924, 2015.

[19] M. Ojaroudi, C. Ghobadi, and J. Nourinia, "Small square monopole antenna with inverted T-shaped notch in the ground plane for UWB application," *IEEE Ant. Wireless Prop. Lett.*, vol. 8, pp. 728-731, 2009.

[20] CST Microwave Studio, ver. 2013, Dassault Systems, 10 rue Marcel Dassault, CS 40501, Vélizy-Villacoublay Cedex, France, 2013.

[21] A. Conn, N.I.M. Gould, and P.L. Toint, *Trust-region methods*, MPS-SIAM Series on Optimization, Philadelphia, 2000.

[22] S. Koziel and A. Bekasiewicz, "Expedited simulation-driven design optimization of UWB antennas by means of response features," *Int. J. RF Microwave CAE*, vol. 27, no. 6, pp. 1-8, 2017.